THE JOURNAL OF PHYSICAL CHEMISTRY B

Article

pubs.acs.org/JPCB

Competing Specific Interactions Investigated by Molecular Dynamics: Analysis of Poly(*p*-dioxanone)/Poly(vinylphenol) Blends

Inger Martínez de Arenaza, Natalia Hernandez-Montero, Emilio Meaurio,* and Jose-Ramon Sarasua*

Department of Mining-Metallurgy Engineering & Materials Science, School of Engineering, University of the Basque Country (UPV/EHU), Alameda de Urquijo s/n. 48013 Bilbao, Spain

ABSTRACT: Molecular dynamics simulations (MD) were carried out to model the miscibility behavior of blends of poly(*p*-dioxanone) (PPDO) with poly(vinylphenol) (PVPh). The Hildebrand solubility parameters of the pure polymers and the Flory−Huggins interaction parameters of the blends at different compositions were computed. Negative interaction parameters were found across the whole range of compositions, suggesting the miscibility of the system, in agreement with the experimental results. The interaction parameter obtained from melting point depression studies was also found to be in good agreement with the value computed from the simulations. The repeat unit of PPDO contains one ether and one ester group, and both can act as hydrogen bond acceptors. The radial distribution functions (RDFs) between those groups and the hydroxyl groups of PVPh were computed to investigate the competence between the acceptor groups for the specific interactions. The RDFs indicate that interassociation occurs mainly with the ester groups, which is detrimental to the ether groups. This result was also corroborated by the analysis of the hydroxyl stretching region of the blends using Fourier transform infrared spectroscopy (FTIR). The good overall agreement found between the simulated and the experimental data reveals the importance of the molecular modeling techniques in the analysis of the miscibility behavior of polymer blends.

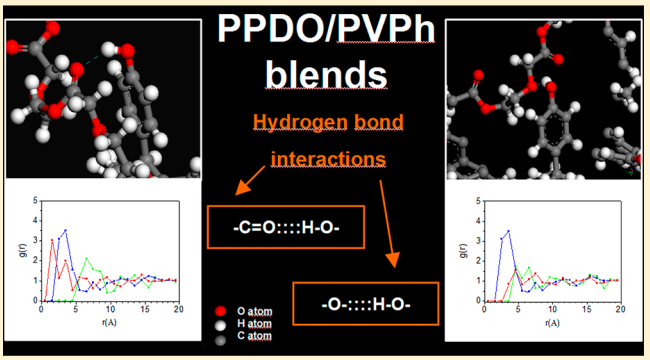

1. INTRODUCTION

Poly(*para*-dioxanone) (PPDO) is a poly(etherester) containing one ether and one ester group per repeat unit, endowing it with outstanding characteristics such as mechanical flexibility, biodegradability, and biocompatibility.[1−3] These properties made PPDO suitable to be used in common medical devices for controlled drug delivery, tissue engineering, and bone fracture fixation. However, its high cost and relatively fast degradation rate[4] have hindered its commercial applications. Therefore, blending PPDO with other polymers is a relatively simple and convenient way to modify its properties and to overcome the drawbacks mentioned above. A candidate polymer to improve the properties of the PPDO is poly(4-vinylphenol), (PVPh), an amorphous polymer with high glass transition temperature. PVPh is a hydrogen bond donor amenable to form miscible blends through the establishment of strong hydrogen bonding interactions with polymer partners carrying acceptor groups in its repeat unit.[5,6]

Molecular Dynamics simulation (MD) is considered one of the most valuable tools to study the phase behavior of polymer blends because the miscibility of any system can be investigated without the need of performing any experimental measurement, and even without the need of synthesizing the investigated polymers. In recent years, MD simulations have reached a high level of sophistication, up to the point of being able to readily predict several important properties with high accuracy,[7] anticipating therefore the possible applications of the modeled systems.[8] These calculations are assumed to bring polymeric systems close to their thermodynamically realistic states. The most important relevance of MD in the study of polymer blends is the analysis of the miscibility of the system. Once realistic blend cells have been built, they can be used to analyze several properties of the new material, such as its mechanical properties or its permeability to gases, following the same procedures as that for pure polymers.

Due to the small mixing entropy contribution, miscibility at the molecular level is not easily obtained in polymer blends. Hence, traditional experimental methods[9−13] can be advantageously replaced by computational methods[14,15] in several scenarios, for example, to avoid the synthesis of difficult to obtain polymers or to avoid interfering effects occurring during the preparation of the mixture, such as melt degradation processes or phase separation through the $\Delta\chi$ effect during casting processes. PVPh has been already investigated using modeling techniques; however, such studies have not been carried out with PPDO or its blends.

The aim of this work is to investigate the miscibility behavior of PPDO/PVPh blends using MD. According to a recent investigation,[16] this system is completely miscible and is able to establish a complex interacting pattern because in addition to

Received: October 18, 2012
Revised: December 16, 2012
Published: December 18, 2012

the hydroxyl−hydroxyl autoassociation interactions, it can also present two types of interasssociation contacts, hydroxyl−carbonyl and hydroxyl−ether interactions. Considering that the experimental determination of the nature of the interactions responsible for the miscibility in such a complex system is far from being straightforward, we are interested in its analysis using molecular modeling techniques. This paper consists of two parts, (1) the modellization of the PPDO/PVPh blends via MD and (2) the validation of the results against experimental data. The nature of the interactions present in the modeled systems has been analyzed by computing selected radial distribution functions (RDFs), and these calculations have been compared with the experimental results obtained using Fourier transform infrared (FTIR) spectroscopy. In addition, the calculated Flory−Huggins interaction parameter has been compared with the one that was obtained using melting point depression studies for PPDO rich blends.[16]

2. EXPERIMENTAL PART AND SIMULATION DETAILS

2.1. Materials. PPDO (Resomer X 206 S; intrinsic viscosity 1.5−2.2 dL/g at 0.1% in HFIP, 30 °C) was supplied by Aldrich Chemical Corp. (Spain). PVPh with an average molecular weight (M_w) of 25.000 g/mol was purchased from Aldrich Chemical Corp. Blends of PPDO with PVPh covering the whole composition range were obtained by solvent casting at 70 °C from 1,4-dioxane solutions containing 10 wt % polymer blends. The cast films were dried at 60 °C in a vacuum oven for 24 h to remove any residual solvent.

2.2. Differential Scanning Calorimetry (DSC). The DSC measurements were performed with a DSC Q200 Modulated from TA Instruments. The weight of the samples varied between 5 and 10 mg, and two consecutive scans were performed at a heating rate of 20 °C/min up to 250 °C (to ensure the complete melting of the sample) under a nitrogen atmosphere. For melting point depression studies, samples were allowed to crystallize isothermally until crystallization was complete, and they were then heated with a scan rate of 5 °C/min to obtain the melting point values for pure PPDO and for the PPDO/PVPh blends.

2.3. Fourier Transform Infrared Spectroscopy (FTIR). FTIR spectra of the blends were recorded on a Nicolet AVATAR 370 spectrophotometer. The spectra were obtained at room temperature with 2 cm^{-1} resolution, averaging 64 scans in the range of 4000−450 cm^{-1}. Blend films were prepared by casting the 1,4-dioxane solutions containing the polymer blends on KBr pellets at 70 °C. Then, the samples were vacuum-dried at 60 °C for 24 h.

2.4. Simulation Details. Molecular modeling simulations were accomplished using Discover and Amorphous Cell modules of the Materials Studio (MS) software suite (version 4.1) provided by Accelrys (San Diego, U.S.A.). Amorphous Cell module employs the combined use of the arc algorithm developed by Theodorou and Suter[17] and the scanning method of Meirovitch.[18]

The amorphous cells were constructed with MS Visualizer building tools in cubic unit cells with periodic boundary conditions. Initial structures were constructed with Flory's rotational isomeric state (RIS) model that describes the conformations of the unperturbed chains.[19] Mixture cells where the chains were "well mixed" were chosen,[8] that is, with an acceptable number of intermolecular contacts, avoiding the excessive overlaps and the unoccupied spaces between chains. Then, the conjugate gradient method (CGM) was selected to minimize its energies with a convergence level of 10^{-3} kcal/mol.

All of the simulations were performed with the condensed-phase optimized molecular potentials for atomistic simulation studies (COMPASS) force field. In the COMPASS approach, the total energy of the system can be expressed as a sum of valence (or bond) ($E_{valence}$), cross-term ($E_{cross\text{-}term}$), and nonbond interaction energies ($E_{nonbond}$), given as

$$E_{total} = E_{valence} + E_{cross\text{-}term} + E_{nonbond} \quad (1)$$

The valence energy ($E_{valence}$) corresponds to energies associated with bond stretching, valence angle bending, dihedral angle torsion, and inversion, also called the out-of-plane interaction energy. Moreover, it includes a new term named Urey−Bradley.[14] In addition, the cross-term energy ($E_{cross\text{-}term}$) introduces correction factors to the valence energy, such as the bond−bond energy term that considers stretch−stretch interactions between two adjacent bonds. It also includes stretch−bend, bend−bend, stretch−torsion, bend−torsion, and bend−bend−torsion terms. Finally, the nonbond interactions ($E_{nonbond}$), defined as the sum of the van der Waals energy, the Coulomb electrostatic energy, and the hydrogen bond energy, are calculated using the cell multipole method. The van der Waals energy, described by the Lennard-Jones (LJ) 6−12 potential, and the electrostatic interactions, defined by Coulomb energy terms were calculated by the Ewald summation method,[20] with an accuracy of 10^{-4} kcal/mol and an update width of 5 Å. The partial charges of the atoms in the systems were estimated by the charge-equilibration method.[21] After construction and minimization, the cells were refined by MD simulations, consisting of the equilibration for 200 ps at 298 K with time steps of 1 fs in the *NVT* ensemble.

3. SIMULATION RESULTS

Initially, different short chains of both polymers were constructed. Afterward, the Hildebrand solubility parameters, δ, of the built polymers were calculated in order to obtain a description of the attractive strength between the molecules in the system. The solubility parameter is defined as the square root of the cohesive energy density, (CED), or the cohesive energy (E_{coh}) per unit volume, as described in eq 2.

$$\delta = \sqrt{\mathrm{CED}} = \sqrt{\frac{E_{coh}}{V}} \quad (2)$$

One of the most important choices is the number of repeat units of the polymer chains in the modeled cubic cells. Because longer chains increase the computation times, the objective of this first step is choosing the minimum chain length presenting intermolecular interactions of similar strength to those occurring in the high-molecular-weight polymer chain. This representative length can be determined by calculating the solubility parameter for chains of different size and choosing the length above which the solubility parameter attains a constant value. Figure 1 shows that the calculated solubility parameter of both polymers has unsteady values when the molecular weight is too small. Furthermore, the trend of the solubility parameter of PVPh is less obvious due to the autoassociation of the hydroxyl groups.[14] As can be seen, at least 10 repeat units are necessary to achieve a nearly constant calculated solubility parameter for both polymer chains.

Table 1 summarizes the main characteristics of the pure polymers, detailing their molecular weights (M_w) and the

dx.doi.org/10.1021/jp310340v | J. Phys. Chem. B 2013, 117, 719−724

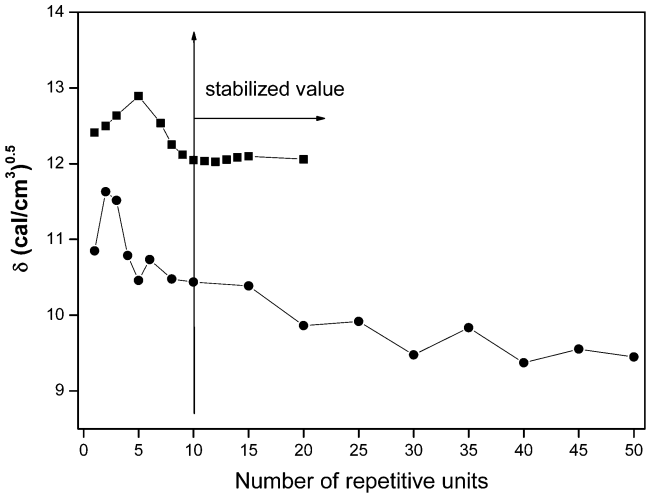

Figure 1. Evolution of the calculated solubility parameters of (■) PPDO and (●) PVPh with molecular weight.

solubility parameters computed from MD simulations (δ_{MD}) and from alternative methods (δ_{exp}). The experimental solubility parameter of PPDO, $\delta_{expPPDO}$, is unreported and has been therefore estimated using the group contribution method proposed by Small.[22] On the other hand, $\delta_{expPVPh}$ has been determined using solubility testing experiments.[23] The solubility parameters calculated using MD (δ_{MD}) show negative deviations compared to the experimental values. This behavior was observed in several polymers such as PLLA, PDLA, PS, and PVPh. Initially, this effect was attributed to the low molecular weight of modeled polymers; however, other authors reported the same phenomenon for PVPh despite using large and complex models for the simulation.[24−26]

In order to evaluate the miscibility of the PPDO/PVPh mixtures, the free energy of mixing, ΔE_{mix}, has been determined for the investigated blend cells and for the pure polymers.[27] The free energy of mixing per unit volume is given by eq 3.

$$\Delta E_{mix} = \phi_A\left(\frac{E_{coh}}{V}\right)_A + \phi_B\left(\frac{E_{coh}}{V}\right)_B - \left(\frac{E_{coh}}{V}\right)_{mix} \quad (3)$$

where ϕ_A and ϕ_B represent the volume fractions of the two polymers in the blend (PPDO and PVPh). According to the Flory−Huggins theory, the interaction parameter, χ_{AB}, of the blends can be calculated from ΔE_{mix} according to the following equation:

$$\chi_{AB} = \left(\frac{\Delta E_{mix}}{RT\phi_A\phi_B}\right)V_r \quad (4)$$

where V_r is the reference molar volume, R is the molar gas constant, and T is the temperature.

In addition, the actual parameter indicating the miscibility of the blends is the critical value of the Flory−Huggings interaction parameter, $(\chi_{AB})_{critical}$, defined according to eq 5.

$$(\chi_{AB})_{critical} = \frac{1}{2}\left(\frac{1}{\sqrt{m_A}} + \frac{1}{\sqrt{m_B}}\right)^2 \quad (5)$$

where, m_A and m_B represent the degree of polymerization of the neat polymers, actually the number of repeat units (in this case, $m_A = m_B = 10$), resulting in $(\chi_{AB})_{critical} = 0.20$. If χ_{AB} is smaller than $(\chi_{AB})_{critical}$, the system is completely miscible. However, if χ_{AB} is only slightly larger than the critical value, the system exhibits partial miscibility, in which phase separation occurs only within a certain compositional range, and both phases contain non-negligible amounts of the second component. For larger values of χ, the system is completely immiscible. Therefore, by comparing the values of χ_{AB} with $(\chi_{AB})_{critical}$, the miscibility behavior of the system can be predicted.

The sizes of the cubic cells for the modeled blends were calculated from the densities of the individual polymers at room temperature (ρ_{PPDO} = 1.344 g/cm^3, ρ_{PVPh} = 1.25 g/cm^3),[28,29] assuming the rule of mixtures. The molar volumes ($V_m = M/\rho$) were obtained from the molecular weights of the repeat units and the densities of the neat polymers, resulting in 75.9 cm^3/mol for PPDO and 96.0 cm^3/mol for PVPh. Figure 2 shows the

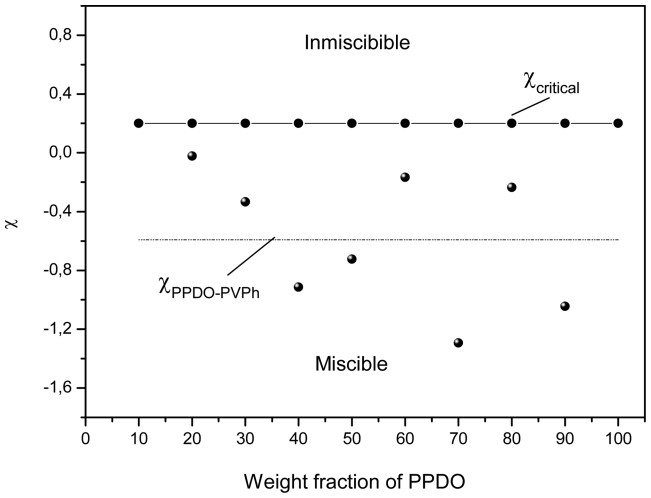

Figure 2. Flory−Huggins interaction parameters of the mixtures versus the wt % of PPDO in the blend.

calculated Flory−Huggins interaction parameter for different blend compositions. The scatter of the calculated data can be attributed to the limited size of the cells, and the average value for the interaction parameter is $\chi_{AB} \approx -0.6$. Nevertheless, because the value of χ_{AB} is always below the critical value, it can be concluded that the molecular modeling simulation of the PPDO/PVPh blends predicts complete miscibility in the whole range of compositions. Figure 3 shows the PPDO/PVPh 1/4 blend composition after minimization and refinement by MD calculations.

The miscibility of the PPDO/PVPh blends can be attributed to hydrogen bonding interactions between the functional groups of the two polymers. However, in this case, the repeat

Table 1. Details of Pure PPDO and PVPh Polymers Studied by MD Simulation

pure polymers	acronyms	repeat units	M_w (g/mol)	δ_{MD} (cal/cm^3)$^{0.5}$	δ_{exp} (cal/cm^3)$^{0.5}$
poly(*p*-dioxanone)	PPDO	10	1020	12.0	13.4
poly(vinylphenol)	PVPh	10	1200	10.4	12.0

dx.doi.org/10.1021/jp310340v | J. Phys. Chem. B 2013, 117, 719−724

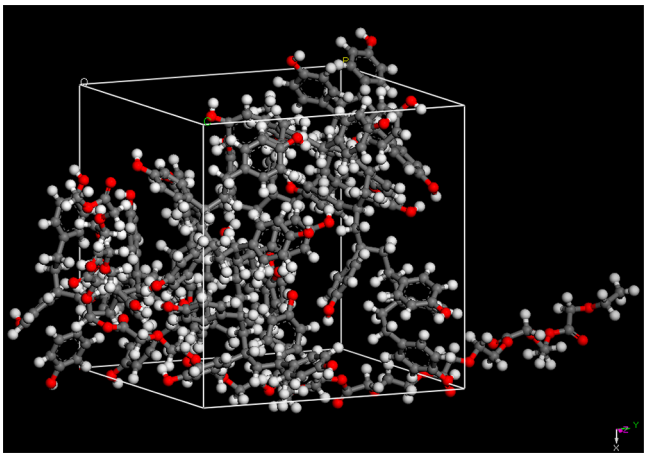

Figure 3. Snapshot of an amorphous unit cell containing 1/4 chains of PPDO/PVPh blends. The red color represents oxygen, the gray carbon, and the white hydrogen atoms.

unit of PPDO contains two acceptor groups, the carbonyl (>C═O) and the ether (−O−) group, both of them amenable of interacting with the hydroxyl groups (−OH) of PVPh. The analysis of the RDF obtained from the molecular models can provide insight about the contribution of each group to the overall interassociating interactions.[30] This analysis is usually carried out in terms of the pairwise RDF, $g(r)$, that gives the probability of finding an atom (or functional group or molecule) a distance r from another atom (or functional group or molecule) compared to the ideal gas distribution.[31] This pair distribution function is therefore dimensionless and tends to unity at infinite distance.

Figure 4 shows the pair distribution functions, $g(r)$, computed for the hydroxyl group pairs in neat PVPh (Figure 4a), the ether group pairs in neat PPDO (Figure 4b), and that for the hydroxyl−carbonyl pairs (Figure 4c) and the hydroxyl−ether pairs (Figure 4d) in the PPDO/PVPh 1/2 blend. As can be seen in Figure 4a, PVPh shows a large peak at about 3 Å, indicative of the hydroxyl−hydroxyl autoassociation in PVPh. In this case, the DRF has been obtained analyzing the distances between the hydrogen atoms located in the hydroxyl groups of PVPh, and the peak distance indicates the most probable distance between the H atoms located in the hydrogen-bonded hydroxyl−hydroxyl pairs. On the contrary, the RDF obtained for the ether atoms in neat PPDO (Figure 4b) indicates a random distribution of these atoms in the bulk because no clear peak is present. The small peaks observed can be attributed deviations from the true statistical distribution arising from the limited size of the models.

The PPDO/PVPh 1/2 blend contains identical total amounts of both donor and acceptor groups and has been therefore used to investigate the RDFs corresponding to the specific interactions expected to occur in the blends. Figure 4c displays the RDFs calculated using the carbonyl oxygens and the hydroxyl hydrogens for the PPDO/PVPh 1/2 blend. As can be seen (red curve) the hydroxyl−carbonyl interassociation shows a peak located at about 2.0 Å, indicative of the occurrence of −OH···O═C interactions. In addition, the peak corresponding to the hydroxyl−hydroxyl autoassociation (blue curve) is still present, but its height decreases noticeably (from about 4.5 to about 3.5) upon going from neat PVPh to the blend, indicating the reduction of the autoassociation extent upon blending.[32] Moreover, the RDFs corresponding to the carbonyl oxygens (green curve) show no definite peak,

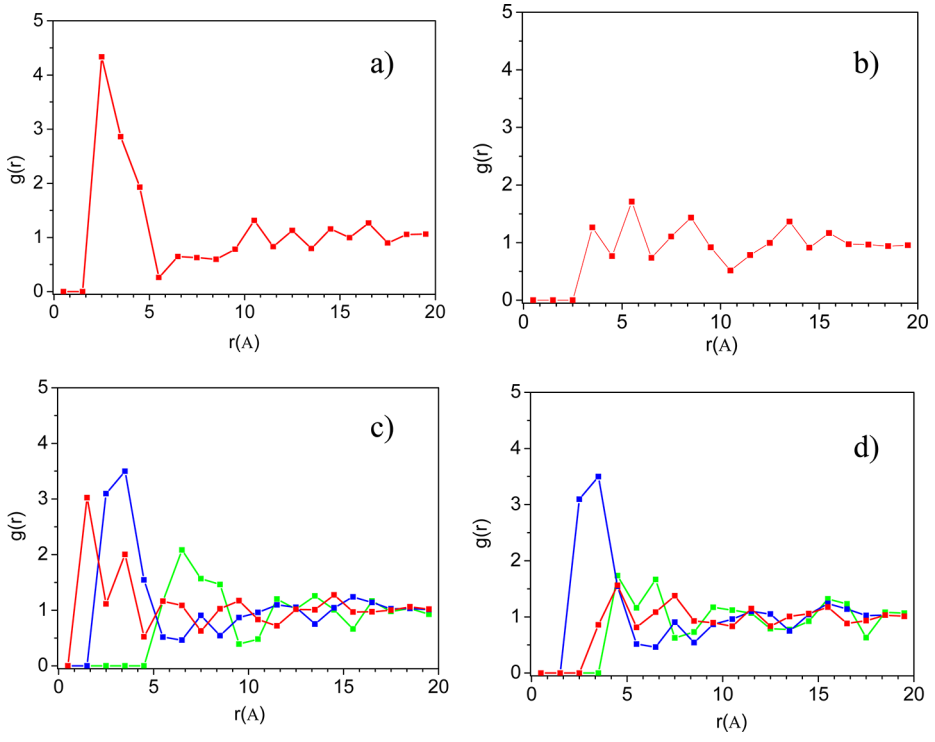

Figure 4. RDFs for (a) hydroxyl−hydroxyl autoassociation in neat PVPh (b) ether−ether autoassociation in neat PPDO, (c) hydroxyl−carbonyl interassociation (red), hydroxyl−hydroxyl autoassociation (blue), and carbonyl−carbonyl autoassociation (green) in the PPDO/PVPh 2/1 blend, and (d) hydroxyl−ether interassociation (red), hydroxyl−hydroxyl autoassociation (blue), and ether−ether autoassociation (green) in the PPDO/PVPh 2/1 blend.

dx.doi.org/10.1021/jp310340v | J. Phys. Chem. B 2013, 117, 719−724

indicating the lack of carbonyl−carbonyl autoassociation. Finally, Figure 4d displays the RDFs calculated using the ether oxygens and the hydroxyl hydrogens for the PPDO/PVPh 1/2 blend. As can be seen, the RDF corresponding to the interassociation (red curve) is null up to a value of about 3.0 Å, above the sum of the VDW radii of H and O (1.2 and 1.5 Å, respectively), proving the absence of hydroxyl−ether hydrogen bonding interactions in the PPDO/PVPh 1/2 blend investigated in this paper. In summary, molecular modeling results indicate that interassociation occurs predominantly between the hydroxyl and the carbonyl groups, the the extent of the hydroxyl−ether interactions being negligible.

4. VALIDATION OF THE MODELING ANALYSIS: COMPARISON WITH EXPERIMENTAL RESULTS

The PPDO/PVPh system has been recently investigated by our research group,[16] and in this section, we will only deal with the experimental results relevant to the validation of the molecular modeling results already presented in this paper. The DSC curves of pure PPDO and PVPh were found to show T_g's at −8 and 156 °C, respectively, and the DSC traces of the blends showed single T_g's intermediate between those of the pure polymers, indicating the miscibility of the system,[33] in agreement with the modeling results. In addition, the depression of the equilibrium melting point was analyzed using the Nishi−Wang equation,[34] originally based on the Flory−Huggins theory,[35] to obtain the Flory−Huggins interaction parameter. The Hoffman−Weeks method[36] was used in this treatment to obtain the equilibrium melting points. Crystallization of PPDO was only observed within the range of compositions from 100/0 to 80/20, and the experimental polymer−polymer interaction parameter was $\chi_{AB} = -1.0$. This moderately negative value confirms a thermodynamically miscible blend[33] and is in reasonable agreement with the value obtained using molecular modeling simulations ($\chi_{AB} = -0.6$), supporting the predictive ability of these methods. The difference between the calculated and the experimental result can be explained considering two main sources of error; first, force fields are usually parametrized seeking good agreement with selected properties, among which the cohesive energy density is not usually included because it is not easily accessible (see also the discussion of Table 1 in section 3). However, the fact that ΔE_{mix} is obtained from eq 3 as the cohesive energy density difference between identical calculation volumes points fortunately to an important error cancellation, although some remnant systematic error is to be expected. Second, the blend cells investigated in this paper contain between 307 (1:1 mol blend) and 995 atoms (1:5 mol blend) in order to speed up the MD calculations. The limited size of the cells is mainly responsible for the dispersion of the calculated data around the mean value (errors of mainly random nature; see Figure 2).

More interestingly, the specific interactions present in the PPDO/PVPh blends have been investigated by FTIR.[6,37] Particularly, the location of the OH stretching band is related to the strength of the hydrogen bonding interactions. Figure 5 shows the OH stretching region for PVPh and PPDO/PVPh blends of different composition. Pure PVPh shows a broad, complex band due to the addition of contributions arising from a wide number of different species,[9,38] including hydroxyl−π interactions, hydroxyl dimers, and hydroxyl multimers of different length. This band is centered at about 3360 cm^{-1}, a location associated therefore to the dominating species in pure PVPh, the hydroxyl multimers. Upon mixing with PPDO, the

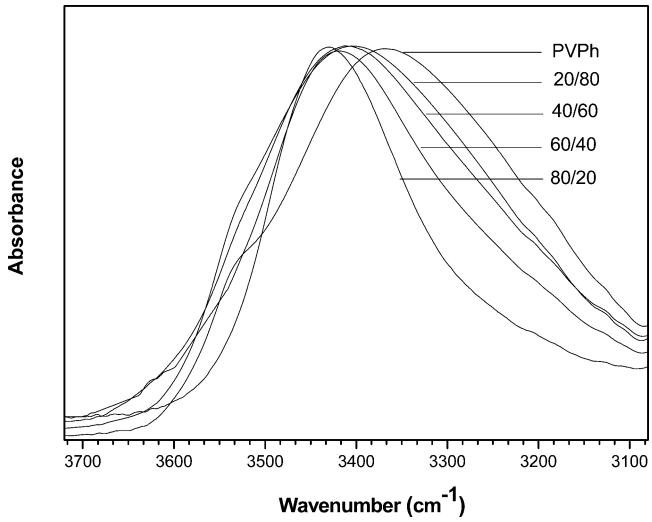

Figure 5. Hydroxyl stretching region for pure PVPh and PPDO/PVPh blends of different compositions.

maximum of the OH stretching band shifts to higher frequencies up to about 3420 cm^{-1} in the case of the PPDO/PVPh 80/20 blend, a location that can be attributed to the interassociation interactions. The question arising here is whether PPDO contains two different functional groups, the ether group and the carbonyl ester, amenable to acting as hydrogen bond acceptors. We have therefore compared our FTIR results with those reported in the literature to gain insight into the nature of the interactions (see ref 31 for further details). When PVPh is blended with polyethers (such as poly(vinylmethylether), poly(vinylethylether), or poly(tetrahydrofurane)),[39,40] the hydroxyl stretching band corresponding to the interassociation interactions is located at about 3320 cm^{-1}, while blending PVPh with polyesters (such as poly(vinylacetate), poly(methylmethacrylate), poly(ε-caprolactone), or poly(3-hydroxybutyrate)) leads to an interassociation band located at about 3440 cm^{-1}. Because the location observed in Figure 5 for the interassociation interactions (3420 cm^{-1}) is closer to the typical location corresponding to O−H···O═C hydrogen bonds (3440 cm^{-1}) than to the typical location reported for O−H···O− hydrogen bonds (3320 cm^{-1}), it can be concluded that interassociation interactions in PPDO/PVPh blends are mainly hydroxyl−carbonyl contacts, detrimental to the hydroxyl−ether interactions. This result is also in very good agreement with the RDFs obtained in the modeling simulations.

5. CONCLUSIONS

The miscibility of PPDO/PVPh blends has been investigated using MD simulations, and the calculated results have been compared with the experimental data. Modeling analyses predict the miscibility of the system, and there is good agreement between the interaction parameter obtained from molecular modeling simulations ($\chi_{AB} = -0.6$) and the experimental value ($\chi_{AB} = -1.0$). In addition, both molecular modeling simulations and the analysis of the specific interactions by FTIR indicate that the interassociation interactions are responsible for the miscibility take place mainly between the hydroxyl groups of PVPh and the carbonyl groups of PPDO, while hydroxyl−ether interactions show minor importance. MD simulations successfully model polymer

dx.doi.org/10.1021/jp310340v | J. Phys. Chem. B 2013, 117, 719−724

blends with competing interassociating interactions, such as those occurring in the PPDO/PVPh system.

AUTHOR INFORMATION

Corresponding Author

*Fax: +34-94-601-3930. E-mail: emiliano.meaurio@ehu.es (E.M.); jr.sarasua@ehu.es (J.R.S.).

Notes

The authors declare no competing financial interest.

ACKNOWLEDGMENTS

The authors are thankful for funds of the Basque Government, Department of Education, Universities and Research (GIC10/152-IT-334-10) and Dept. of Industry (IE10/276), and MICINN (BIO2010-21542-C02-01). I.M.A. and N.H.M. thank the University of the Basque Country (UPV-EHU) for a pre-doctoral grant.

REFERENCES

(1) Yang, K. K.; Wang, X. L.; Wang, Y. Z. *J. Macromol. Sci., Polym. Rev.* **2002**, *C42* (3), 373−398.
(2) Bai, W.; Zhang, Z.; Li, Q.; et al. *Polym. Int.* **2009**, *58* (2), 183−189.
(3) Zeng, J.-B.; Zhu, Q.-Y.; Li, Y.-D.; Qiu, Z.-C.; Wang, Y.-Z. *J. Phys. Chem. B* **2010**, *114* (46), 14827−14833.
(4) Zhou, Z. X.; Wang, X. L.; Wang, Y. Z.; et al. *Polym. Int.* **2006**, *55* (4), 383−390.
(5) Qiu, Z.; Komura, M.; Ikehara, T.; Nishi, T. *Polymer* **2003**, *44* (26), 8111−8117.
(6) Iriondo, P.; Iruin, J. J.; Fernandez-Berridi, M. J. *Macromolecules* **1996**, *29* (17), 5605−5610.
(7) *Accelrys Software*; Accelrys Software Inc.: San Diego, CA, 2004.
(8) Jawalkar, S.; Adoor, S.; Sairam, M.; Nadagouda, M.; Aminabhavi, T. *J. Phys. Chem. B* **2005**, *109* (32), 15611−15620.
(9) Meaurio, E.; Zuza, E.; Sarasua, J. R. *Macromolecules* **2005**, *38* (4), 1207−1215.
(10) Meaurio, E.; Zuza, E.; Sarasua, J. *Macromolecules* **2005**, *38* (22), 9221−9228.
(11) Zuza, E.; Meaurio, E.; Etxeberria, A.; Sarasua, J. *Macromol. Rapid Commun.* **2006**, *27* (23), 2026−2031.
(12) Zuza, E.; Lejardi, A.; Ugartemendia, J. M.; Monasterio, N.; Meaurio, E.; Sarasua, J. R. *Macromol. Chem. Phys.* **2008**, *209* (23), 2423−2433.
(13) López-Rodríguez, N.; López-Arraiza, A.; Meaurio, E.; Sarasua, J. R. *Polym. Eng. Sci.* **2006**, *46* (9), 1299.
(14) Martinez de Arenaza, I.; Meaurio, E.; Coto, B.; Sarasua, J. R. *Polymer* **2010**, *51* (19), 4431−4438.
(15) Martinez de Arenaza I.; Meaurio E.; Sarasua J. R. Analysis of the Miscibility of Polymer Blends through Molecular Dynamics Simulations. In *Polymerization*; De Souza Gomes, A., Ed.; InTech: Croatia, 2012, ISBN: 978-953-51-0745-3.
(16) Hernandez-Montero, N.; Meaurio, E.; Elmiloudi, K.; Sarasua, J. R. *Eur. Polym. J.* **2012**, *48* (8), 1455−1465.
(17) Theodorou, D.; Suter, U. *Macromolecules* **1985**, *18* (7), 1467−1478.
(18) Meirovitch, H. J. *Chem. Phys.* **1983**, *79* (1), 502−508.
(19) Flory, P. J.*Statistical Mechanics of Chain Molecules*; Hanser: Munich, Germany, 1989.
(20) Ewald, P. P. *Ann. Phys.* **1921**, *369* (3), 253−287.
(21) Rappe, A.; Goddard, W. J. *Phys. Chem.* **1991**, *95* (8), 3358−3363.
(22) Small, P. *J. Appl. Chem.* **1953**, *3* (2), 71−80.
(23) Arichi, S.; Himuro, S. *Polymer* **1989**, *30* (4), 686−692.
(24) Jawalkar, S. S.; Raju, K. V. S. N.; Halligudi, S. B.; Sairam, M.; Aminabhavi, T. M. *J. Phys. Chem. B* **2007**, *111* (10), 2431−2439.
(25) Mu, D.; Huang, X.; Lu, Z.; Sun, C. *Chem. Phys.* **2008**, *348* (1−3), 122−129.
(26) Gestoso, P.; Brisson, J. *Comput. Theor. Polym. Sci.* **2001**, *11* (4), 263.
(27) Case, F. H.; Honeycutt, J. D. *Trends Polym. Sci.* **1994**, 259−66.
(28) Nishida, H.; Yamashita, M.; Endo, T.; Tokiwa, Y. *Macromolecules* **2000**, *33*, 6982−6986.
(29) Gestoso, P.; Brisson., J. *Polymer* **2003**, *44* (8), 2321−2329.
(30) Jawalkar, S. S.; Aminabhavi, T. M. *Polymer* **2006**, *47* (23), 8061−8071.
(31) Horta, A.; Freire, J. J. *Polymer* **2004**, *45* (4), 1275−1286.
(32) Moolman, F. S.; Meunier, M.; Labuschagne, P. W.; Truter, P. *Polymer* **2005**, *46* (16), 6192−6200.
(33) Utracki, L. A. *Polymer Blends Handbook*; Springer-Verlag: New York, 2002; Vol. *1*−*2*.
(34) Nishi, T.; Wang, T. *Macromolecules* **1975**, *8*, 909−915.
(35) Flory, P. J. *Principles of Polymer Chemistry*; Cornell University Press: New York, 1953.
(36) Hoffman, J. D.; Weeks, J. J. *J. Res. Natl. Bur. Stand.* **1962**, *66A*, 13.
(37) Braun, D.; Böhringer, B.; Eidam, N. *Polym. Bull.* **1989**, *21*, 63−68.
(38) Wang, J.; Cheung, M. K.; Mi, Y. *Polymer* **2002**, *43* (4), 1357−1364.
(39) Moskala, E. J.; Varnell, D. F.; Coleman, M. M. *Polymer* **1985**, *26* (2), 228−234.
(40) Landry, M. R.; Massa, D. J.; Landry, C. J. T.; et al. *J. Appl. Polym. Sci.* **1994**, *54* (8), 991−1011.